

STUDY ON VORTEX STRUCTURE OF JETS THROUGH REMOTE SENCING

By

Sotoaki Onishi

Professor , Department of Civil Engineering,
Science University of Tokyo Noda, Chiba, Japan

SYNOPSIS

Fluid dynamic characteristics of water jets in field are discussed applying remote sensing techniques including aerial photography, infrared photography, echo sounding and the Landsat data. Tidal currents in the Naruto are selected as the object of the study, because the currents present typical appearance of the water surface jets. The dynamic characteristics of the jets to be discussed include coherent structure of vortices in shear layers, structure of potential core, circulation, vertical profiles of the vortices, preferred mode of the jets and behaviour of the jets in far field.

INTRODUCTION

Fluid dynamic characteristics of jets have been one of interesting topics relating to turbulent flow and studied by many researchers. But almost all existing results have been on the basis of either theoretical or experimental investigation. In this paper, the author tries to investigate the deterministic features of non-buoyant surface jets with application of several remote sensing techniques including aerial photography, infrared photography as well as radio echo sounding.

Tidal currents flowing the Naruto strait will be selected as the object of the study. Onishi and Nishimura (4) and Maruyasu, Onishi and Nishimura (3) have previously investigated characteristics of the vortices along shear layers formed on both sides of the jets flows, revealing roles of the vortices on the mass exchange through the strait.

In this paper, the author will consider the tidal currents as typical examples of the water surface jet and discuss its hydrodynamic features such so called "preferred mode" of oscillation in the shear layers, vertical profiles of the turbulent vortices, vortex strength and so on.

FIELD OBSERVATION OF VORTEX STRUCTURE

Fig. 1 indicates schematic diagram of the turbulent jet flow produced by the

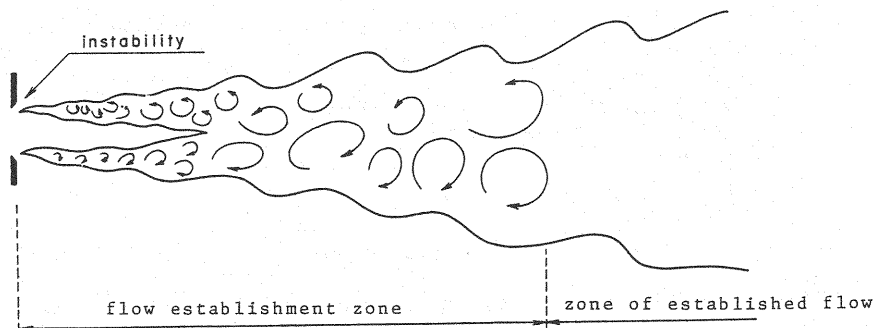


Fig. 1 Schematic diagram of the turbulent jets

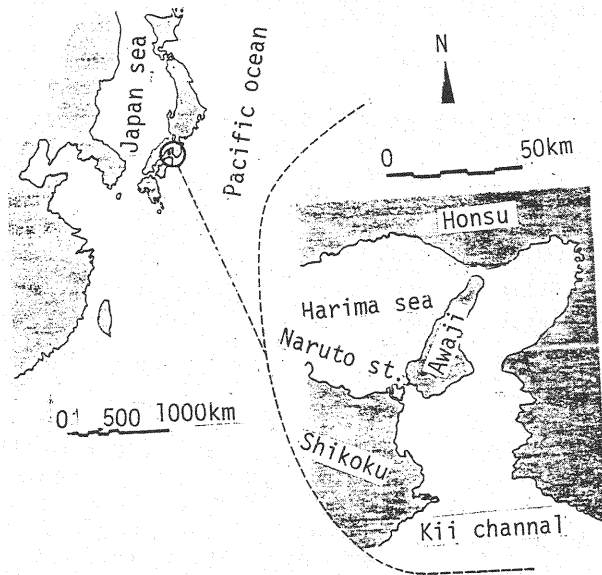


Fig. 2. Location of the Naruto st.

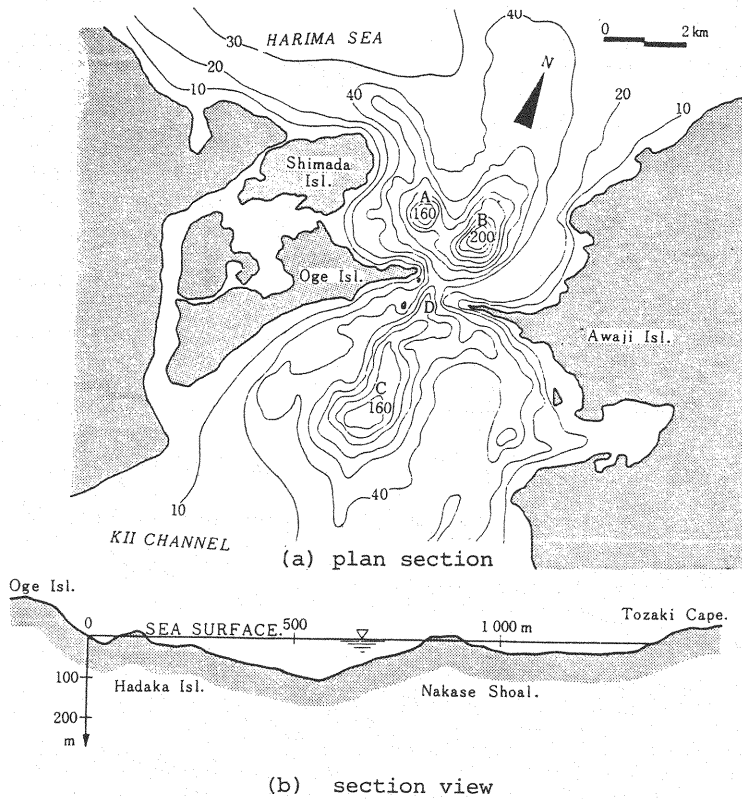


Fig. 3. Bottom configuration of the Naruto strait

water exiting through a narrow strait into a semi-infinite ocean, in which the flow region is divided into the zone of flow establishment and the zone of established flow. Firstly, we will pay attention to the former, of which special feature is existence of a potential core. In the Naruto strait, we can observe a typical example of the zone of flow establishment. The Naruto strait is located in the eastern part of the Seto Inland sea, coastal zone of which is one of the most industrialized area in Japan (Fig. 2). The width of the strait is about 1,100 meter and the maximum depth is more than 80 meter at its centre section. Fig. 3 indicates sea bottom configuration around the strait. A distinguished feature of the strait is the existence of fast tidal current.

Tidal level each side of the strait ebbs and rises periodically with a period of about 12 hours. The tidal current is caused by the difference of these tidal levels. At spring tide its difference reaches about 1.5 meter and causes the flow velocity of about 10 knots.

Photo. 1 is an example of the aerial photograph of the Naruto strait at an altitude of about 1,000 meter, representing a stage of the southward tidal flow of 9.1 knots flowing from Harima Sea into the Kii Channel. In the photo, one can see a series of vortices along a pair of the shear layers. Although such shear layers are widely considered as consisting of many vortices of various diameters, the vortices in Photo. 1 seem to have coherent structure and spread out over whole width of the shear layers. Interval of neighbouring vortices increases in the downstream region. It has been said by Winnant and Browand (6) that such turbulent vortices of the organized structure are formed through rapid coalescing of the neighbouring two or more vortices with smaller scale. Photo. 2 is another example of the aerial photograph obtained at lower altitude of 600 meter and presents more clearly the vortex coalescing.

As mentioned above, the horizontal distribution of the vortices in the turbulent shear layers can be easily observed in field by the aerial photograph. On the other hand, although vertical profiles of the vortices should be an interesting subject to be observed in the field, any conventional measurement method can not provide it. But application of the echo sounding seems to be a way to overcome this difficulty. Its principle is similar to those used in marine acoustic sounding; in essence, acoustic waves emitted into water body are reflected on the sea bottom and at air bubbles or suspending dirts in and around the vortices and then difference of the reflectance is displayed by difference of colour. Photo. 3 represents some examples of the results, in which (a) shows profiles of the vortices in a region of about 14 meter water depth along the shear layer in the right side facing downstream, (b) profiles in other region of about 8 meter depth a little further downstream and (c) those further downstream of the above two. In Photo.3(a), one can see vortices stretching downwards from the water surface and also a wedge-like water body rising from the sea bottom, indicating existence of upwelling current around the vortex. Photo.3(c) shows profiles of vortices of a relatively larger scale distributing along the shear layer in the water region of about 52 meter depth. Again, they reach the sea bottom. Neither the weaker vortices (Photo.3(d)) nor the vortices just after finishing the coalescence in Photo. 3(e) reach the sea bottom as far as the echo sounding can indicate, against the principle of preservation of the circulation in the potential flow theory. Finally, Photo. 3(f) indicates the results obtained along a course traversing the current from Shikoku to Awaji, in which the maximum water depth is about 22 meter.

On the basis of the field observations, the author thinks that the turbulent vortices in the shear layers of the tidal current in the strait have columnlike coherent structure reaching from the water

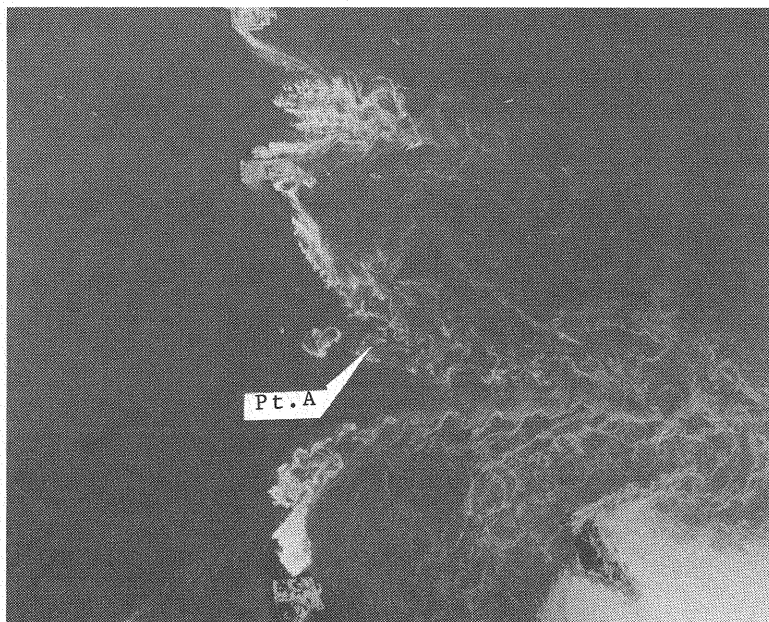


Photo. 1. Aerophoto of southward current (9.1 knots)
in the Naruto strait

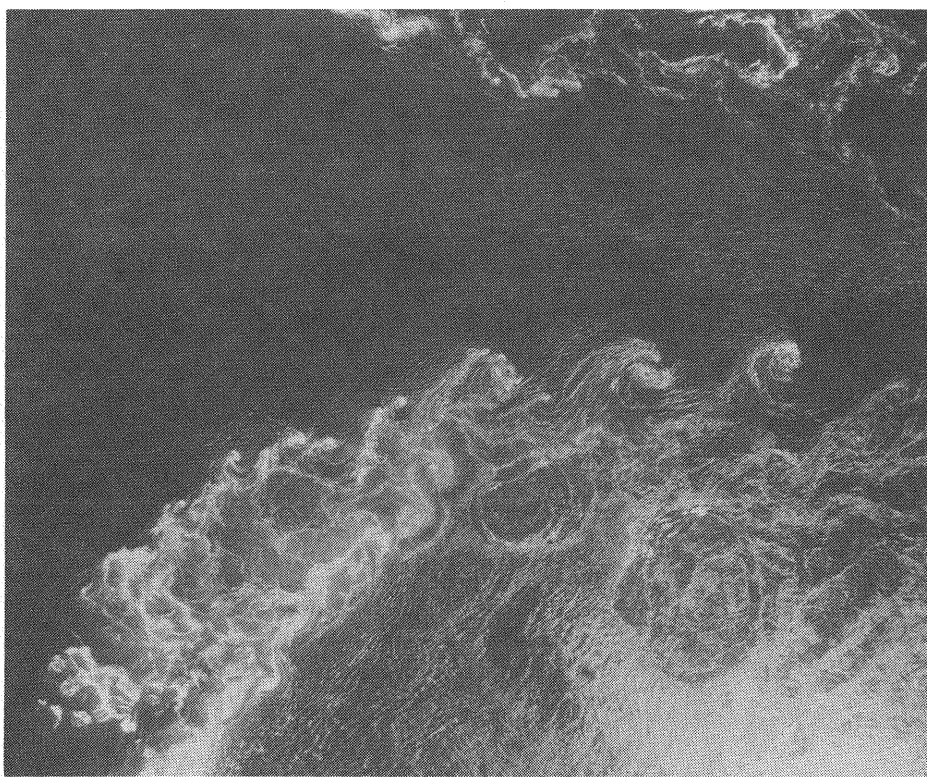


Photo. 2. Growing process of vortices

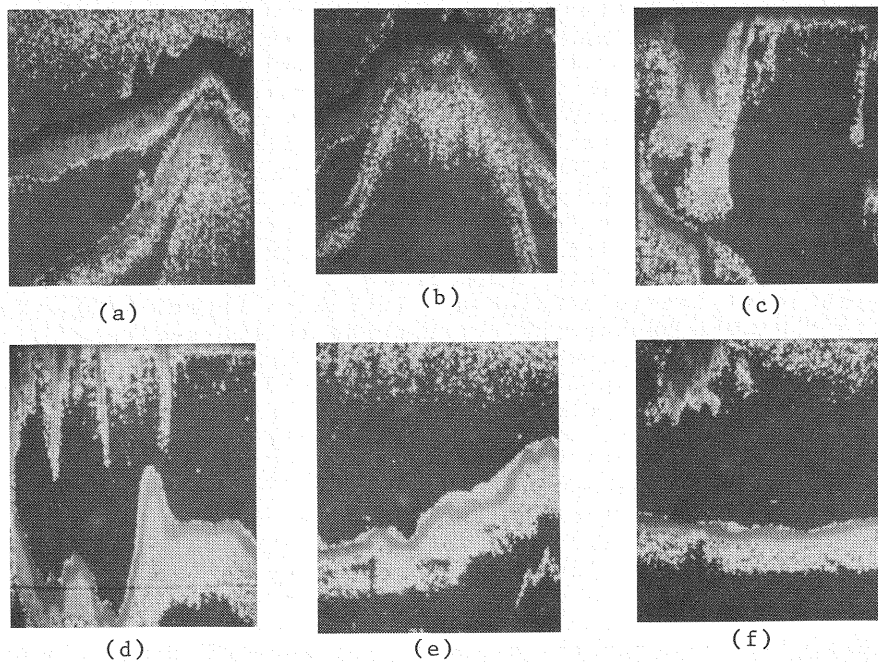


Photo. 3. Vertical profiles of vortices in the Naruto strait

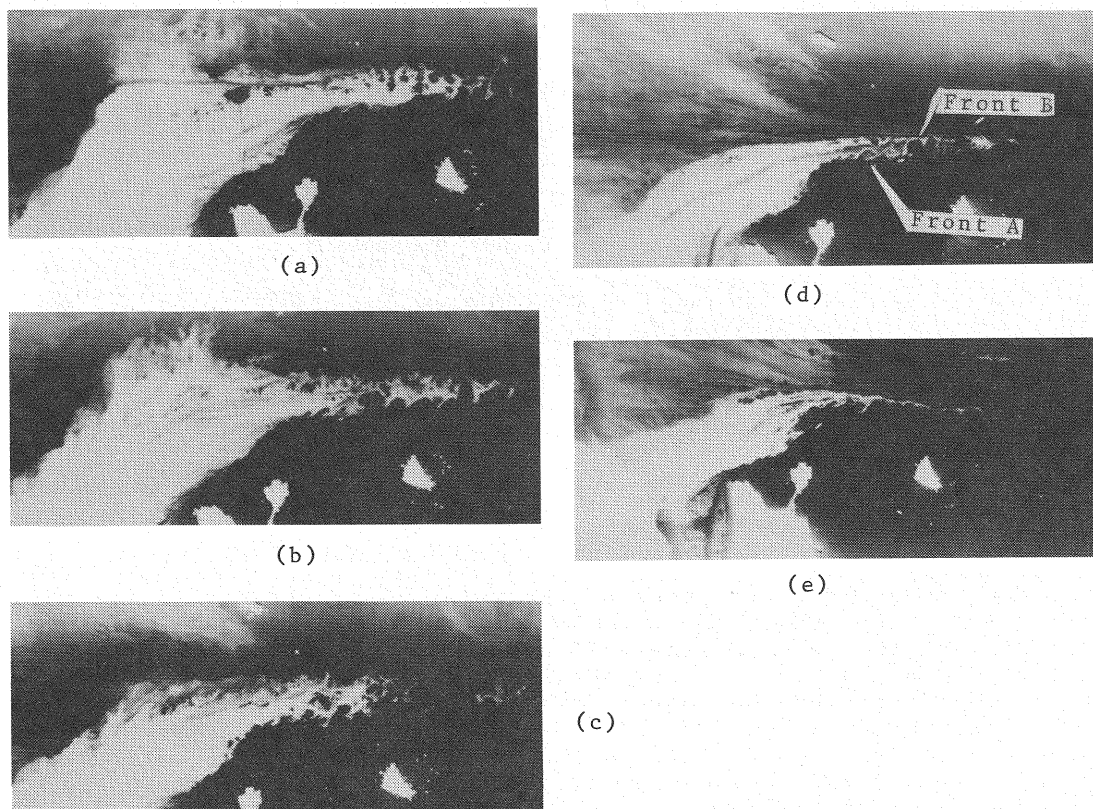


Photo. 4. Thermal images of southward current in the Naruto
(flight height is 600 meter)

surface to the sea bottom.

Another interesting subject on the zone of flow establishment is to observe the structure of the potential core in the field. In this study, this is done by using the infrared photography. Photo. 4 (a) through (e) are thermal images taken at an altitude of 600 meter at 11:1 A.M. ((a)), that is, 30 minutes before the maximum southward flow condition, 11:16 A.M. ((b)), 11:25 A.M. ((c)), 11:38 A.M. ((d)) and 11:46 A.M. ((e)), respectively, on 16th of July 1977. Darker tone of the images indicates lower temperature at the surface water. A warmer water body passing through the strait shows that the potential core is being divided into two regions along the centre of the main flow. The division is denoted as Front B in Photo. 4(d). Front A noted in the same photograph corresponds to the series of the vortices along the shear layers, which indicate typical appearance of Kelvin-Helmholtz type. In the classical potential flow theory, it has been said that the velocity distribution in the potential core should be uniform. But in Photo. 4, a series of small circular spots similar to rollers can be observed along the centre line of the main flow and also one can see that the rollers are especially prominent in Photo. 4 (a), when the tidal current is weaker. With increase of flow velocity, those circular spots are destroyed and finally disappear. Indeed, if the stress along the shear layers is weaker, the unstable waves take a shape of a series of circular spots instead of Kelvin-Helmholts.

Next, let our concerns shift to the zone of established flow. Photo. 5 is the thermal image obtained at 4,000 m altitude at 11:02 A.M. on Aug. 23rd 1979. The tidal condition at the time is 30 minutes after the slack from the northward to the southward flow.

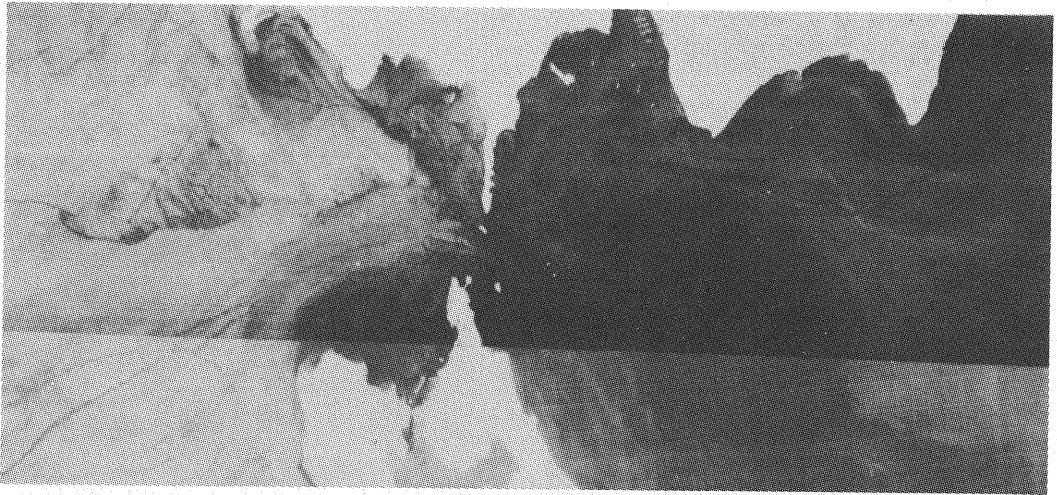


Photo.5. Thermal image of the southward current.
(flight hight of 4,000 m, Aug. 23rd,1979)

The homogeneous dark tone of the water mass suggests that a strong mixing took place during the passage through the strait. Horizontal spreading of the jets is linear if effect on the fluid viscosity is neglected. However, in actual jets in natural water region the jet width is affected by the bottom friction and aspect ratio of the exit as well as bottom slope, as indicated in Fig. 4, in which f , b , h_0 and k denote friction factor, half width of the jet exit, water depth in the exit and the bottom slope, respectively. In the figure the author's experimental results together with analytical results by Ozzoy and Unluata (5) are plotted. In Photo. 5, we can see that the jets in the Naruto strait are affected by these parameters.

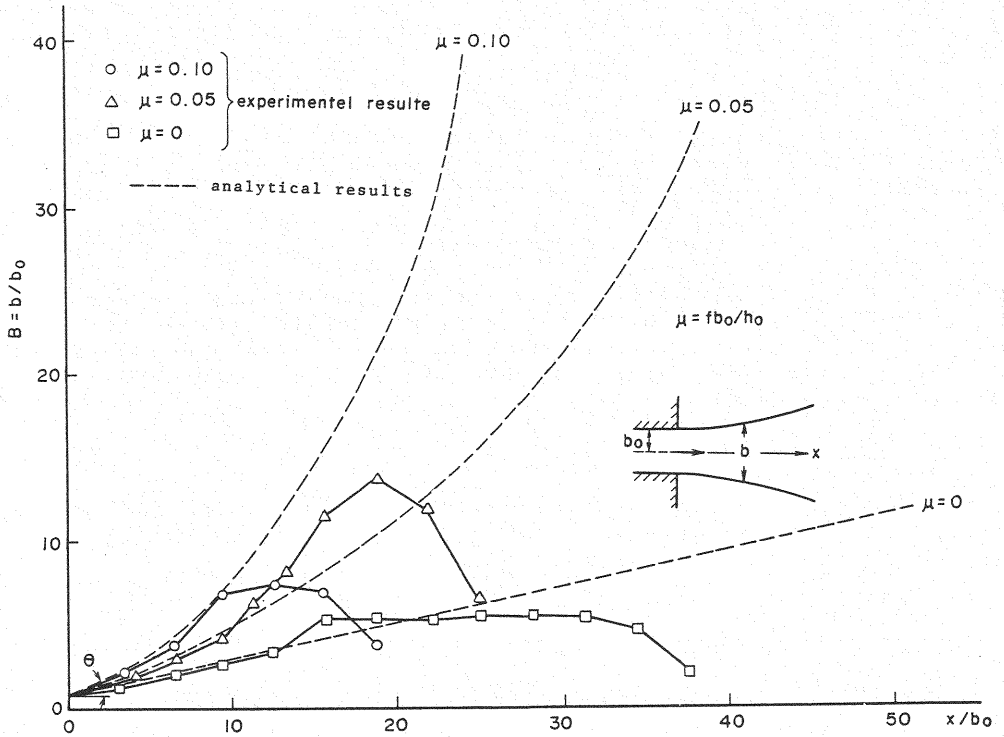


Fig. 4. Effects of bottom roughness and aspect ratio on the jet width in homogeneous fluid

FIELD OBSERVATION OF VORTEX STRENGTH

Referring to Fig. 5 and assuming that vorticity generated at the point P is preserved during transportation to downstream direction along the shear layer, vorticity flux passing through section I in a unit time can be estimated as follows.

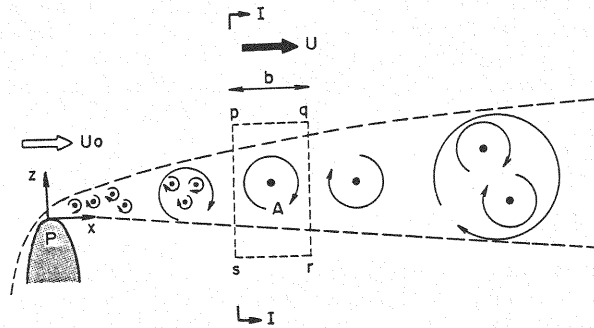


Fig. 5. Schema of the coalescing of vortices

Volume flux of the fluid passing through an element of thickness dy in the unit time is Udy , where U is velocity in the direction normal to y -axis. Vorticity ω in the fluid of the unit volume is

$$\omega = dU/dy \quad (1)$$

Therefore, vorticity flux, ωf_{lux} passing through the section I becomes

$$\omega f_{lux} = \int_{-\infty}^{\infty} U \omega dy = \int_{-\infty}^{\infty} \frac{dU}{dy} U dy = \frac{1}{2} U^2 \quad (2)$$

With assumption that the shear layers consist of coherent vortices, each of which is distributed in a constant interval of d and possesses a propagating velocity of c , strength of each vortex F becomes

$$F = (\omega f_{lux}) t = \frac{1}{2} (U^2) \frac{d}{c} \quad (3)$$

where, t denotes time interval of vortex generation and equal to b/c . Thus, once U , d , c can be measured in the field, the vortex strength can be estimated by a method based on water surface depression.

Assuming a line vortex as shown in Fig. 6, the vortex strength can be represented by

$$F = 2\pi R \sqrt{g \Delta h} \quad (4)$$

where, R denotes a radius of irrotational flow region adjacent to the vortex axis, g , the gravitational acceleration and Δh , the surface water depression at the axis of vortex.

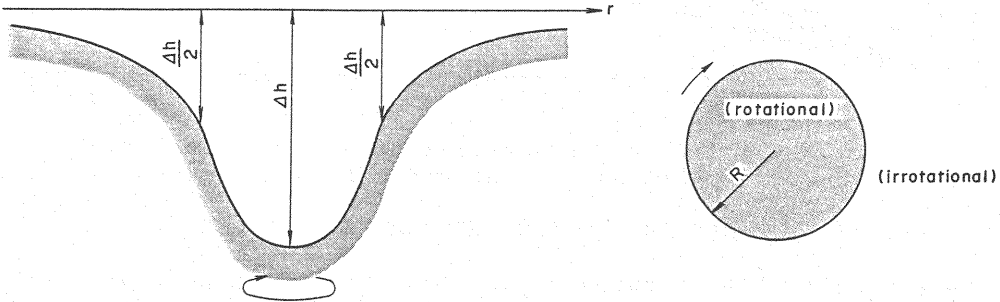


Fig. 6. Vortex model

With the above relation, one can obtain the vortex strength if value of R and Δh are measured in the field. Spatial intervals and propagating velocity of vortices are observed by the aerial photographs taken in certain time intervals. Maruyasu, Onishi and Nishimura (3) tried such observations in the strait with time interval of three seconds, on April 1st 1977, July 2nd 1977, March 8th 1977 and February 24th 1978.

To measure the current velocity, application of the principle of Kameron effect is useful; suppose a water particle at the water surface flowing with velocity to the same direction as that of the aeroplane, one can see that the displacement of the water particle in the time interval produces an illusion a relative height when viewed through a stereoscope. Therefore, the velocity of the water particle can be observed through a stereoplotter. As a results, contour maps showing velocity distributions can be obtained. Fig. 7 is an example of this kind.

Table. 1. Strength of the "Vortex of Naruto"

| Date | Vortex No. | U_0 (m/sec) | x (m) | d (m) | c (m/sec) | τ (sec) | F (m ² /sec) |
|-------------------|------------|------------------|------------|------------|----------------|-----------------|------------------------------|
| 1977 Apr. 1st | 1 | 3.7 | 100 | 17 | 2.1 | 8 | 60 |
| | 2 | — | 120 | 28 | 3.1 | 9 | 60 |
| | 3 | — | 160 | 63 | 4.2 | 15 | 100 |
| | 4 | — | 240 | 90 | 3.8 | 24 | 160 |
| | 5 | — | 340 | 96 | 4.6 | 36 | 240 |
| | 6 | — | 440 | 163 | 4.0 | 41 | 280 |
| | 1' | — | 170 | 73 | 3.5 | 21 | 140 |
| | 2' | — | 240 | 74 | 2.9 | 25 | 270 |
| | 3' | — | 320 | 66 | 2.1 | 32 | 220 |
| | 4' | — | 380 | 86 | 3.3 | 26 | 180 |
| | 5' | — | 490 | 129 | 4.6 | 28 | 190 |
| | 6' | — | 630 | 143 | 4.2 | 34 | 230 |
| 1977 Jul. 2nd | 1 | 4.1 | 150 | 80 | 3.9 | 21 | 170 |
| | 2 | — | 230 | 74 | 4.0 | 19 | 160 |
| | 3 | — | 300 | 66 | 3.5 | 19 | 160 |
| | 4 | — | 360 | 80 | 3.3 | 24 | 200 |
| | 5 | — | 460 | 96 | 4.5 | 21 | 180 |
| 1977 Mar. 8th | 1 | 4.4 | 100 | 58 | 2.5 | 23 | 220 |
| | 2 | — | 160 | 59 | 3.4 | 17 | 170 |
| | 3 | — | 220 | 64 | 2.8 | 23 | 220 |
| | 4 | — | 290 | 73 | 2.5 | 29 | 280 |
| | 5 | — | 360 | 114 | 4.1 | 28 | 270 |
| | 1' | — | 160 | 58 | 2.9 | 20 | 190 |
| | 2' | — | 220 | 76 | 2.8 | 27 | 260 |
| | 3' | — | 310 | 70 | 3.0 | 23 | 230 |
| | 4' | — | 360 | 84 | 2.7 | 31 | 300 |
| | 5' | — | 480 | 123 | 3.0 | 41 | 390 |
| 1978 Feb. 24th | 1 | 4.55 | 120 | 44 | 2.8 | 16 | 160 |
| | 2 | — | 160 | 52 | 4.2 | 12 | 130 |
| | 3 | — | 220 | 86 | 4.7 | 18 | 190 |
| | 4 | — | 340 | 82 | 3.3 | 25 | 260 |
| | 5 | — | 390 | 66 | 3.5 | 19 | 190 |
| | 6 | — | 470 | 100 | 4.0 | 25 | 260 |
| | 1' | — | 280 | 56 | 4.0 | 14 | 140 |
| | 2' | — | 340 | 50 | 3.2 | 16 | 160 |
| | 3' | — | 380 | 48 | 2.8 | 17 | 180 |
| | 4' | — | 430 | 76 | 3.4 | 23 | 230 |
| | 5' | — | 530 | 100 | 5.3 | 19 | 200 |

Vortex No.1, 2, (1', 2') mean the vortex positioned in the right(left) hand free boundary layer; X denotes distance between the numbered vortex and its generated point.

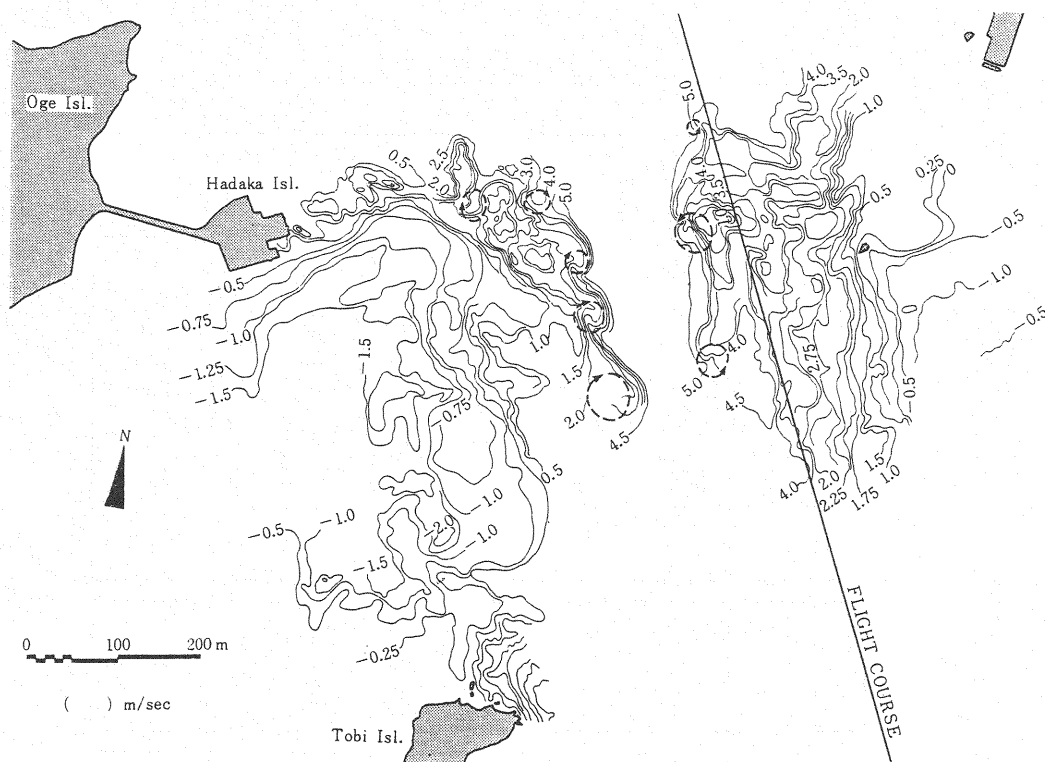


Fig. 7. Contour map of the velocity distribution

Next, water surface depression in Eq. 4 can be measured through synchronously photographing from a pair of airplanes. The sea surface was synchronously photographed in the Naruto strait from the aeroplanes at the altitude of 1,000 meter with 80 % overlap to get a series of synchronized aerial photographs. Each pair of the aerial photographs were analyzed with the A-7 autograph and a contour map of the sea surface was produced.

From the mentioned results of the field observations together with Eq. 3 or Eq. 4, the vortex strength can be calculated. Details of these estimates have previously been reported by Onishi and Nishimura (4). Therefore, only the results are presented here in Table.1, in which one can see that the strength of the vortices in the strait is $F = 1 \sim 3 \times 10^2 \text{ m}^2/\text{sec}$, and also that the velocity of tidal current in the narrowest section of the strait is about 4 m/sec. It is necessary to add a proviso that the values of the vortex strength in Table.1 are based on Eq. 3. On the other hand, Eq. 4 gives the strength of about $150 \text{ m}^2/\text{sec}$ introducing the vortex radius of 8 meter and the water surface depression of about 1.0 meter

PREFERRED MODE OF SURFACE JETS IN THE NARUTO STRAIT

Regarding to the hydrodynamic feature of the tidal current, namely the surface jet, so called "preferred mode" of the jets is quite an interesting subject to be discussed. Related to this problem, it has been reported by Ho and Nosseir (1) that impingement of separated shear layers on solid boundaries generates a feed back mechanism, which sustains oscillations at selected frequencies and makes the shear layers unstable. Owing to the instability of the shear layers, small perturbations in the flow establishment zone are amplified to form vortices of coherent structure, as they travel downstream. The induced force associated with impingement of these vortices on the solid boundary produces an upstream influence that modulates the sensitive

region of the shear layer near separation and then produce new vorticity perturbations. Ho and Nosseir found that if the solid boundary is located about six times an exit diameter downstream from a round nozzle and if Mach number is above approximately 0.7, then a strong resonance would be produced in the flow. Laufer and Monkewitz (2) found that the amplitude of the unstable oscillations are strongly modulated at Strouhal number $St = FD/U = 0.31$, in which F is the frequency and D and U are the nozzle diameter and the exit velocity, respectively. Regarding to the existing studies mentioned above, it is predicted that the vortex coalescing in the shear layers in the water surface jets shall be stimulated intensively under certain flow conditions and that the feed back mechanism will be generated in the surface water jets by intermittent passages of vortices at the end of the potential core, instead of the impingement on the solid boundaries in an air jets. Further, it is predicted that while the shear layers in the air jets become unstable due to the perturbation of pressure, instability in the water jets shall be induced by surface undulation propagating upstream. Therefore, a feedback mechanism should be only in subcritical flow.

On the basis of the above considerations, the prominent vortices in the Naruto strait such as shown in Photo. 1 and Photo.2 can be sustained at the preferred frequencies. Introducing a nozzle width L as a representative length of the flow, exit velocity at the nozzle V as a representative velocity, and a reciprocal of the passage interval of the vortices at the end of the potential core $1/t$ as a representative frequency, Strouhal number St is represented as

$$St = L / V t_0 \quad (5)$$

where, t_0 corresponds approximately to the value of $t = b/c$ at the downstream end indicated in Table.1. Exact determination of the nozzle width of the surface jets in the Naruto strait is rather difficult. But considering that in Photo. 1 the shear layer in the left side facing to the downstream lacks clarity in the downstream region and that there exists shallow projection denoted as Pt.A in Photo. 1., location of the jet nozzle in the strait may be assumed as shown in Fig. 8 and its width of about 120 meter can be measured. Mean water depth in the assumed nozzle section is approximately 100 meter and a cross sectional area of the exit flow is estimated to be about 12,000 m^2 . In the

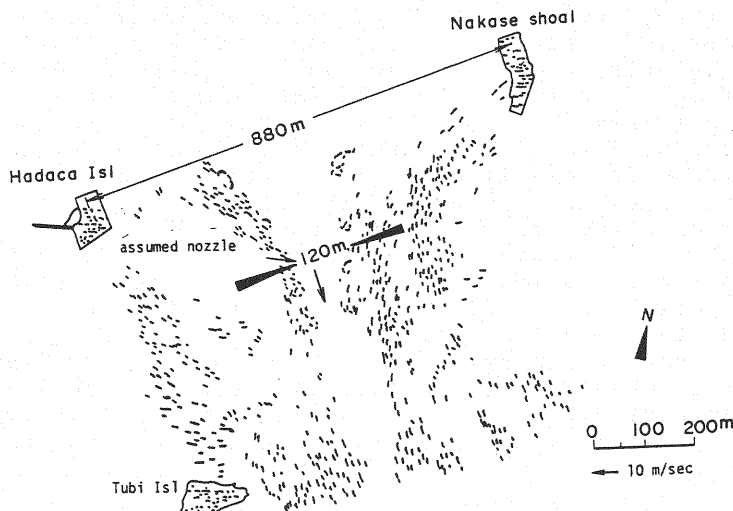


Fig. 8. Assumed location of nozzle in Naruto

section connecting both heads of Oge Island and Tozaki, average velocity of the jets are shown as U_0 in Table 1 and a cross sectional area is about $32,000 \text{ m}^2$. Hence, the principle of continuity gives the exit velocity V in the assumed nozzle section as

$$V = 2.7 U_0 \quad (6)$$

By substituting Eq.6 into Eq.5, Strouhal number becomes

$$St = 44.4 / U_0 t_0 \quad (7)$$

With above relation, Strouhal numbers relating to the vortices along the shear layer in the right side facing to the downstream are calculated and its results are presented in Table.2, in which Strouhal numbers at the end of the potential core in the strait ranges from 0.2 to 0.5. Obtained values have approximately equivalent to those of the

Table. 2. .Estimated Strouhal number of preferred mode in Naruto strait

| Date | Apr. 1st, 1977 | May. 8th 1977 | Jul. 2nd, 1977 | Feb. 24th, 1978 |
|------|----------------|---------------|----------------|-----------------|
| St | 0.22 | 0.25 | 0.51 | 0.30 |

preferred mode in the air jets. This coincidence indicaces that water surface jets are resonant at Strouhal numbers approximately equal to those of the round impinging air jets and also that the shear layers in Photo. 1 are under the condition of the preferred mode.

SUMMARY AND CONCLUDING REMARKS

Hydrodynamic characteristics of the tidal current in the Naruto strait are investigated by introducing the aerial photographic surveying as well as application of the echo sounding from a stand point of the coherent theory of the turbulent flow. Because of the particular geographical features of the strait, tidal currents show typical appearance of the surface jet and the dynamic vortices are produced along the shear layers. With application of stereoscopic photography, the depth of water surface depression at the vortex centre is observed in the Naruto strait. A series of the aerial photograph taken in a fixed time interval are successfully used to obtain various features of these vortices such as the propagating velocity and vortex spacings. From these obtained values of the water surface depression and the propagating velocity as well as the vortex spacings, it is estimated that the vortices along the shear layers in the strait have circulation values of $100 \text{ m}^2/\text{sec}$.

Application of the echo sounding revealed the vertical profiles of the vortices in the field. Its results indicate that turbulent vortices along the shear layers of the tidal currents in the field have a coherent structure resembling column connecting the water surface to the sea bottom. Another interesting results are those regarding to the so called "preferred mode" of the unstable shear layer. Analysis of the field data of the tidal currents in the Naruto strait, the author considers that the dynamic vortices such as shown in Photo. 1 and Photo. 2 are generated along the shear layers due to its instability when Strouhal number at the end of the potential core is in the range of 0.2 to 0.5. These magnitudes of Strouhal number in the preferred mode are approximately equal to those reported in the existing investigations of the air jets.

REFERENCES

1. Ho, C. and N.S. Nossier : Dynamics of an impingement jet, part 1 The feedback phenomenon, *Journal of Fluid Mechanics*, 105, pp.119-142, 1981.
2. Laufer, J. and P. Monkewitz : On turbulent jet flows; A new perspective, AIAA paper 80-0962, Hartford, Conn., 1980.
3. Maruyasu, T., S. Onishi and T. Nishimura : Study on tidal vortex at the Naruto strait through remote sensing, *Bulletin of the Remote Sensing Laboratory, Remote Sensing Series No.1*, Science University of Tokyo, 1981.
4. Onishi, S. and T. Nishimura : Study on vortex current in strait with remote sensing, *Proceedings of the 17th International Conference of Coastal Engineering*, pp.2655-2670, 1980.
5. Ozsoy, C. and U. Unluata : Ebb-tidal flow characteristics near inlets, *Estuarine, Coastal and Shelf Science*, Vol.14, pp.251-262, 1982.
6. Winnant, C.D. and F.K. Browand : Vortex pairing, the mechanism of turbulent mixing layer growth at moderate Reynolds number, *Journal of Fluid Mechanics*, Vol.63, Part 2, pp.237-255, 1973.

APPENDIX - NOTATION

The following symbols are used in this paper:

- | | |
|----------------|---|
| b, b_0 | = half width of jet and half width of jet in exit; |
| c | = propagating velocity of vortex; |
| d | = spacial interval of vortex; |
| F | = vortex strength; |
| f | = friction factor of sea bottom; |
| h, h_0 | = water depth and water depth in jet exit; |
| Δh | = water surface depression at vortex centre; |
| k | = bottom slope; |
| L | = assumed nozzle width in the strait; |
| R | = radius of vortex; |
| St | = Strouhal number of preferred mode of jet; |
| U | = tidal velocity; |
| U_0 | = tidal velocity at the narrowest section in the strait; |
| V | = exit velocity of surface jet in assumed nozzle section; |
| | = vorticity; and |
| $= fb_0 / h_0$ | = parameter reflecting the behaviour of jet in homogeneous fluid, |